

# Circulation

JOURNAL OF THE AMERICAN HEART ASSOCIATION



## **Real-Time Quantification and Display of Skin Radiation During Coronary Angiography and Intervention**

Ad den Boer, Pim J. de Feijter, Patrick W. Serruys and Jos R.T.C. Roelandt

*Circulation* 2001;104:1779-1784

DOI: 10.1161/hc4001.097057

Circulation is published by the American Heart Association, 7272 Greenville Avenue, Dallas, TX 75214

Copyright © 2001 American Heart Association. All rights reserved. Print ISSN: 0009-7322. Online ISSN: 1524-4539

The online version of this article, along with updated information and services, is located on the World Wide Web at:

<http://circ.ahajournals.org/cgi/content/full/104/15/1779>

Subscriptions: Information about subscribing to *Circulation* is online at  
<http://circ.ahajournals.org/subscriptions/>

Permissions: Permissions & Rights Desk, Lippincott Williams & Wilkins, 351 West Camden Street, Baltimore, MD 21202-2436. Phone 410-5280-4050. Fax: 410-528-8550. Email:  
[journalpermissions@lww.com](mailto:journalpermissions@lww.com)

Reprints: Information about reprints can be found online at  
<http://www.lww.com/static/html/reprints.html>

# Real-Time Quantification and Display of Skin Radiation During Coronary Angiography and Intervention

Ad den Boer, BS; Pim J. de Feijter, MD; Patrick W. Serruys, MD; Jos R.T.C. Roelandt, MD

**Background**—Radiographically guided investigations may be associated with excessive radiation exposure, which may cause skin injuries. The purpose of this study was to develop and test a system that measures in real time the dose applied to each 1-cm<sup>2</sup> area of skin, taking into account the movement of the x-ray source and changes in the beam characteristics. The goal of such a system is to help prevent high doses that might cause skin injury.

**Methods and Results**—The entrance point, beam size, and dose at the skin of the patient were calculated by use of the geometrical settings of gantry, investigation table, and x-ray beam and an ionization chamber. The data are displayed graphically. Three hundred twenty-two sequential cardiac investigations in adult patients were analyzed. The mean peak entrance dose per investigation was 0.475 Gy to a mean skin area of 8.2 cm<sup>2</sup>. The cumulative KERMA-area product per investigation was 52.2 Gy/cm<sup>2</sup> (25.4 to 99.2 Gy/cm<sup>2</sup>), and the mean entrance beam size at the skin was 49.2 cm<sup>2</sup>. Twenty-eight percent of the patients (90/322) received a maximum dose of <1 Gy to a small skin area (≈6 cm<sup>2</sup>), and 13.5% of the patients (42/322) received a maximum dose of >2 Gy.

**Conclusions**—Monitoring of the dose distribution at the skin will alert the operator to the development of high-dose areas; by use of other gantry settings with nonoverlapping entrance fields, different generator settings, and extra collimation, skin lesion can be avoided. (*Circulation*. 2001;104:1779-1784.)

**Key Words:** radiography ■ catheterization ■ dosage

Coronary arteriography and x-ray-guided catheter-based interventions are increasingly used. X-ray exposure may be associated with adverse effects, however, as described as early as 1897.<sup>1</sup> Numerous incidents of radiation-induced skin injuries have recently been reported.<sup>2-14</sup> Doses from the prolonged use of fluoroscopy can be very high and place the skin at risk for injury. Even though some modern x-ray equipment uses dose-saving measures, such as added filtration and dose-reducing variable-pulsed fluoroscopy, complicated procedures can still result in high-risk skin doses. It is therefore important to reduce radiation exposure as much as possible.<sup>15-20</sup>

Newer x-ray units have an integrated ionization chamber that allows monitoring of the kinetic energy released in matter (KERMA; the absorbed dose in air)-area product, but the entrance dose and dose distribution at the skin are not indicated. Therefore, there is a need to monitor and to quantify the skin radiation dose.<sup>21-30</sup>

We have developed a system that automatically measures and monitors the accumulated skin radiation dose and allows detection of high-dose areas in real time.

In this study, the feasibility and usefulness of this technique have been investigated by analysis of the frequency distribution of high-dose areas in consecutive patients undergoing percutaneous intracoronary procedures.

## Methods

### Study Patients

The radiation monitoring system was installed in 2 of our interventional laboratories. We were able to collect and analyze complete data from 322 consecutive adult patients (235 men, 87 women; mean age 59 years, range 50 to 69 years). Patient height was 174 cm (range 168 to 180 cm), weight 79 kg (range 70 to 87 kg), and obesity (Quetelet) index 26 (range 24 to 28). Of these, 134 patients underwent a diagnostic procedure and 188 patients an intracoronary intervention (60 patients with a right coronary artery, 75 a left circumflex, and 39 a left anterior descending [LAD] stenosis). Nine patients had bypass grafts, and 5 had a total occlusion.

### Procedures

We developed a mathematical model to calculate the x-ray entrance field and the location of the irradiated areas of the skin. To be able to measure the x-ray dose for each 1 cm<sup>2</sup> of irradiated surface, the following assumptions are made:

1. The patient position (=skin position) is defined by the location of the floating tabletop, and it is further assumed that the patient does not change position during the investigation.
2. Patients are considered to have a circular thorax with a circumference of 90 cm (only adult patients are examined).

The following parameters for radiation monitoring are measured:

1. Table: Patient position and the tabletop (measured in a 3D plane in millimeters, with the floor as reference).

Received May 7, 2001; revision received July 12, 2001; accepted July 31, 2001.

From the Thoraxcenter, Department of Cardiology, Erasmus Medical Center, Rotterdam, Netherlands.

Correspondence to Ad den Boer, Department of Cardiology, Thoraxcenter BD 428, PO Box 2040, 3000 GR Rotterdam, Netherlands. E-mail denboer@card.azr.nl

© 2001 American Heart Association, Inc.

*Circulation* is available at <http://www.circulationaha.org>

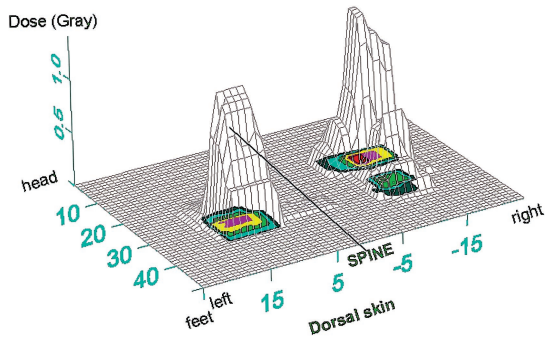


**Figure 1.** Dose distribution at 50×50-cm dorsal skin part after interventional procedure from LAD, followed by implantation of 2 stents. Peak, located at right side, is due to left superior oblique projection, most radiation absorbent projection. Size of high-dose area >1 Gy was 19 cm<sup>2</sup>.

2. Gantry: Rotation and angulation in degrees and source-image distance and isocentric elevation from the floor in millimeters.
3. Collimator: X-ray beam size, horizontal and vertical, in millimeters and the KERMA-area product (KAP; sometimes called dose-area product) value in grays per square centimeters.
4. Generator: X-ray mode and fluoroscopy time (continuous or pulsed) or (digital) cine pulses.

The entrance beam location at the skin was derived from the distance from the x-ray focal spot to the patient in the transverse plane by use of the gantry rotation, focal spot position, and patient position. This distance was corrected for the gantry angulation in the longitudinal plane. The entrance beam size was calculated from the collimator beam dimensions.

The radiation dose at the skin was calculated in grays by use of the entrance beam dimensions and the KAP, measured with an ionization chamber in the collimator.

**TABLE 1. Maximal Possible Beam Size per Image-Intensifier Screen and Skin**

Used image-intensifier field, cm	23	17	13
Maximal beam size at entrance screen, cm	17.9×17.9	13.6×13.6	10.5×10.5
Maximal beam size at skin, cm	9.8×9.8	7.7×7.7	5.9×5.9
Maximal radiated skin area, cm <sup>2</sup>	≈100	≈60	≈35

The theoretical mathematical model is not presented in this article but is available from the authors. The model is used in a monitor system developed by the Siemens Co, the prototype of which is used to retrieve the data.

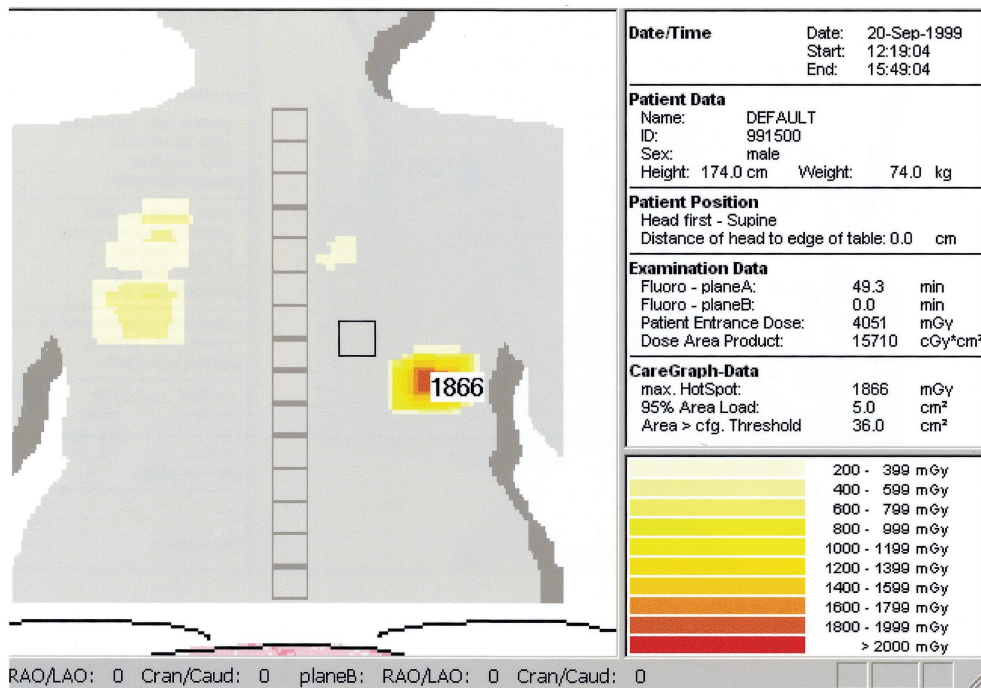
### Graphical Display

Figure 1 shows a 3D graph with the dose distribution at a 50×50-cm dorsal aspect of the skin after an interventional procedure involving the LAD, including implantation of 2 stents. This graph was generated with our prototype system during a pilot study. The graphical display of the system used for data accumulation during our study shows a skin area of 90×90 cm.

Figure 2 is a plot of skin dose depicted in a 2D plane centered over the backbone; the skin surface is virtually split at the sternum and shown laid flat. This graph is automatically displayed on the x-ray monitor after radiation of any part of the skin exceeds a level of 1 Gy. The irradiated skin area is continuously displayed and updated, even when fluoroscopy is not used. This enables the physician to change gantry settings or use extra collimating to avoid possible overlapping with previously irradiated skin parts without using radiation.

### Entrance Beam Dimensions

Both units have automated collimation that limits the beam area to the selected field of view of the image intensifier, independent of



**Figure 2.** Graphical display of prototype system shows skin area of 90×90 cm. Graph is automatically displayed on x-ray monitor after radiation at any part of skin exceeds a level of 1 Gy. Dose report is integrated into this display. Actual irradiated skin area is marked as a square on display (even without fluoroscopy), enabling physician to avoid possible overlap with previously irradiated skin parts by extra collimating or changing gantry settings. Example shows dose distribution at skin after a procedure with 49.3 minutes of radiation time, a PTCA of LAD. Peak entrance dose (hot spot) received by skin was 1.86 Gy to an area of 5.0 cm<sup>2</sup>.

**TABLE 2. Dose Settings of the X-Ray Equipment**

Image-intensifier entrance field size, cm	23	17	13
PFM intensifier dose per image, nGy	10	16	28
PFM intensifier dose per second, $\mu\text{Gy/s}$	0.12	0.20	0.35
DCM intensifier dose per image, nGy	63	104	174

changes in the source-to-image distance (SID tracking). The area of the beam at the skin, however, does change with the source-to-image-intensifier distance. The maximum possible beam areas are given in Table 1.

### Dose Settings of the X-Ray Equipment

The dose settings for the x-ray equipment for the pulsed fluoroscopy mode (PFM) and the digital cine mode (DCM) during the study period are shown in Table 2. The highest possible kilovoltage peak (kVp) during PFM was 110 kVp, and during DCM, 125 kVp. The frequency of PFM was adjusted to 12.5 pulses per second, and the extra beam filter used was 0.2 mm Cu.

The scattered radiation grid had a ratio of 11 and 40 line pairs per centimeter and a focal spot distance of 950 mm and was carbon fiber filled and covered. The radiation measurement was performed with an ionization chamber built into the collimator, and the KAP is shown.

### Statistics

Unless otherwise stated, numerical data are presented as median with interquartile range.

## Results

### Total Radiation Dose per Investigation

The cumulative KAP per investigation was  $52.2 \text{ Gy/cm}^2$  (range 25.4 to  $99.2 \text{ Gy/cm}^2$ ). The mean entrance beam size at the skin was  $49.2 \text{ cm}^2$ , giving an absolute value of 1.06 Gy (Figure 3).

### Radiation Time

The mean fluoroscopy time was 17.8 seconds (range 8.8 to 33.1 seconds), with pulsed fluoroscopy of 12.5 pulses per second. The mean DCM time was 97.9 seconds (range 69.4 to 151.1 seconds), with a frequency of 12.5 frames per second.

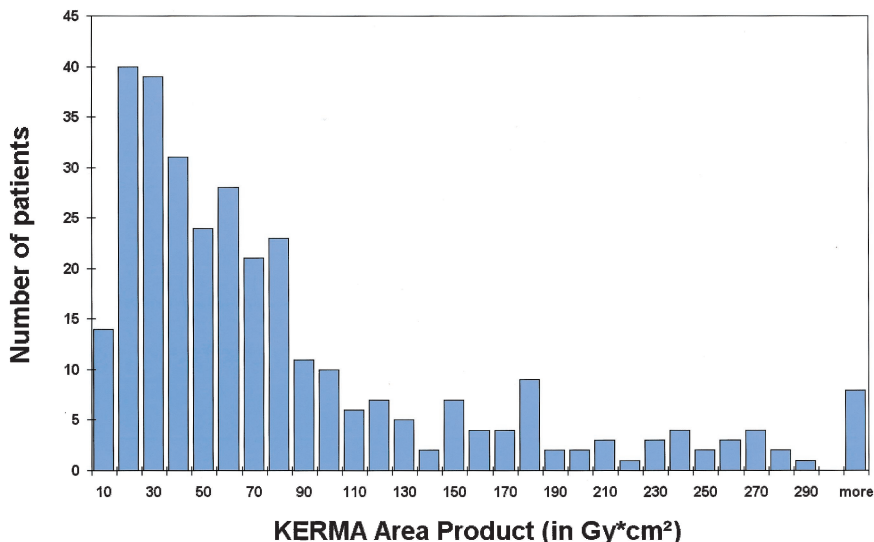


**Figure 3.** KAP measured in 322 patients. Mean value was  $52.19 \text{ Gy/cm}^2$  (range 25.4 to  $99.2 \text{ Gy/cm}^2$ ). Mean size of entrance beam was  $49.2 \text{ cm}^2$ .

### Irradiated Skin Surface

The radiation-exposed skin area in 95% of all investigations was restricted to a size of  $50 \times 50 \text{ cm}$ , including the irradiated area at the groin for catheter introduction and left lateral gantry positioning. This is shown in Figure 1. In the remaining 5% of the cases, the exposed skin area could be visualized by showing a  $90 \times 90\text{-cm}$  area.

### Peak Entrance Dose

The distribution of peak entrance skin doses to the patients in our series is shown in Figure 4. The mean value was  $0.475 \text{ Gy}$ , with a mean area of  $8.2 \text{ cm}^2$  exposed. Dose values  $>1 \text{ Gy}$  occurred in the majority of the patients (52%), whereas parts receiving a dose  $>4 \text{ Gy}$  occurred in only 1.2%. Because our system alerted us in real time when a high-dose area was developing, we were able to avoid excessive dose to that area by changing the gantry settings. It was not necessary to interrupt any procedure as a result of a high-dose “hot spot.”

### Correlation Between the Measured KAP, Patient Obesity, and Fluoroscopy Time

The correlation between the measured KAP and the obesity of the patient, the Quetelet index ( $\text{kg/m}^2$ ), was low ( $R=0.15$ ). Higher doses were correlated with gantry projections that required penetration of thick, highly absorbent body masses. There was a strong relationship between the KAP and fluoroscopy time ( $R=0.78$ ) (Figure 5).

### Correlation Between Measured KAP and Peak Entrance Dose

There was a high correlation between measured KAP and peak entrance dose ( $R=0.89$ ) (Figure 6). We also compared the correlation between KAP and the high-dose areas in the 134 diagnostic and the 188 interventional procedures. The correlation between the interventional procedures ( $R=0.90$ ) was higher than the correlation between diagnostic procedures ( $R=0.35$ ) because of more frequent changing of gantry settings and less overlapping of entrance fields in diagnostic cases.

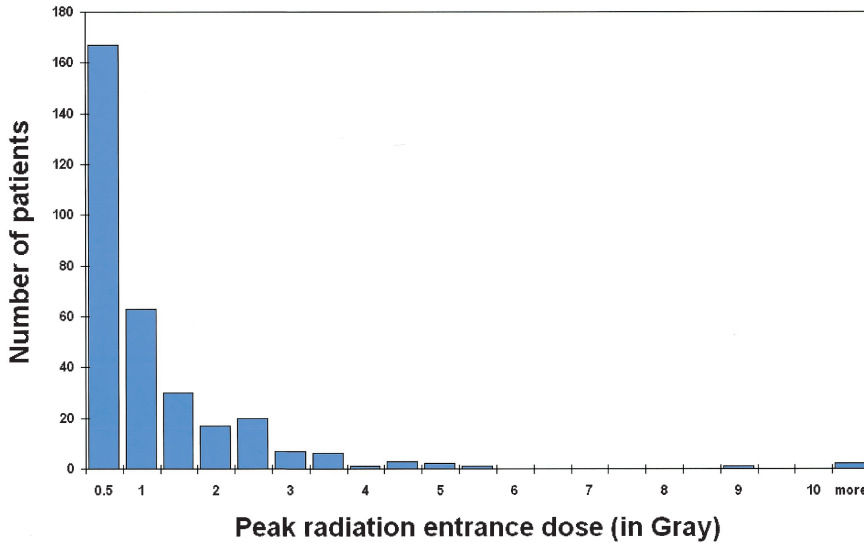


**Figure 4.** Peak entrance dose measured in 322 patients; mean value was 0.475 Gy. Mean size of high-dose area was 8.2 cm<sup>2</sup>.

**Validation of the Measured KAP**

The ionization chamber readings were verified regularly with other measuring devices; the accuracy of the KAP readings was within a 5% range. The values that appear on the monitor reflect the free-in-air KERMA, measured in grays. The dose to the tissue is actually 30% to 40% greater than the value displayed during monitoring, because of backscattered radiation and the KERMA-to-tissue-dose conversion factor.

**Discussion**

Skin injury as a result of radiation exposure was reported as early as 1897.<sup>1</sup> The number of radiologically guided interventions is increasing, as well as the amount of radiation used per procedure. Recent publications show an increasing number of skin injuries during cardiac, abdominal, and neurological interventions.<sup>2-14</sup> High entrance-dose values cannot be avoided in complex investigations, because they often require long exposure times.

Our method allows for skin dose management and makes it possible to keep the dose at a certain skin area as low as reasonable for the procedure. This is important because many

patients have more than one procedure, and skin dose accumulates.

It should be kept in mind that a high dose may produce unacceptable skin damage and should be avoided<sup>26-30</sup> (Table 3). Real-time dose monitoring can prevent these adverse effects because it allows selection of other x-ray techniques, such as extra beam filtering, selection of lower frame rates, and if available, documenting of low-dose fluoroscopic runs during the procedure.<sup>15-18</sup> Extra beam collimation is not often used but is a highly effective way to decrease both patient and operator radiation exposure without loss in image quality.

Finally, the use of other gantry settings allows distribution of the radiation dose over different skin areas and prevents development of a high dose. In our study, only 1.2% of the patients received a dose >4 Gy at some parts of the skin. It should be noted, however, that when equipment without dose-saving measures is used, levels are much higher (up to 7 times).<sup>15</sup>

**Limitations**

The monitoring system used in this study assumed a patient with a thorax circumference of 90 cm. Obviously, this does

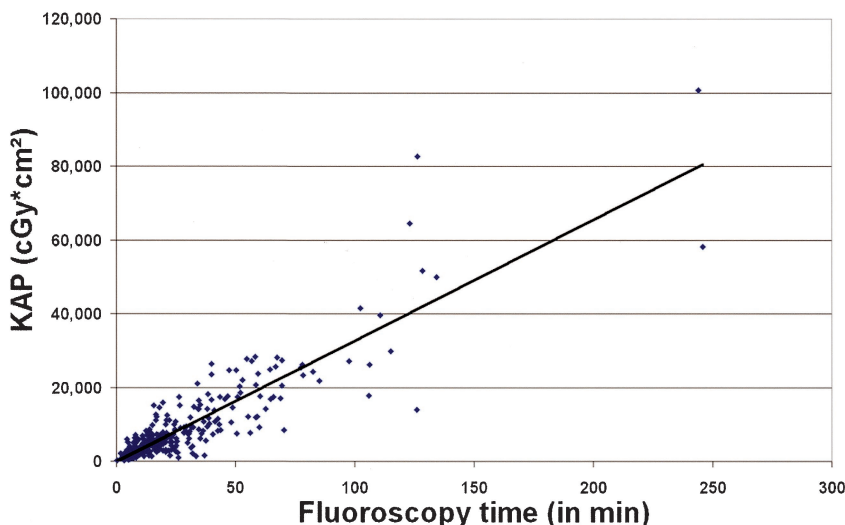


**Figure 5.** Correlation between measured KAP and fluoroscopy time for complete patient group:  $R=0.78$ ,  $x=-75.19$ ,  $y=327.83$ . With extreme values taken out, fluoroscopy times >100 minutes showed  $R=0.70$ ,  $x=537.42$ ,  $y=296.15$ . Mean KAP was 52.19; mean fluoroscopy time used was 17.8 minutes.

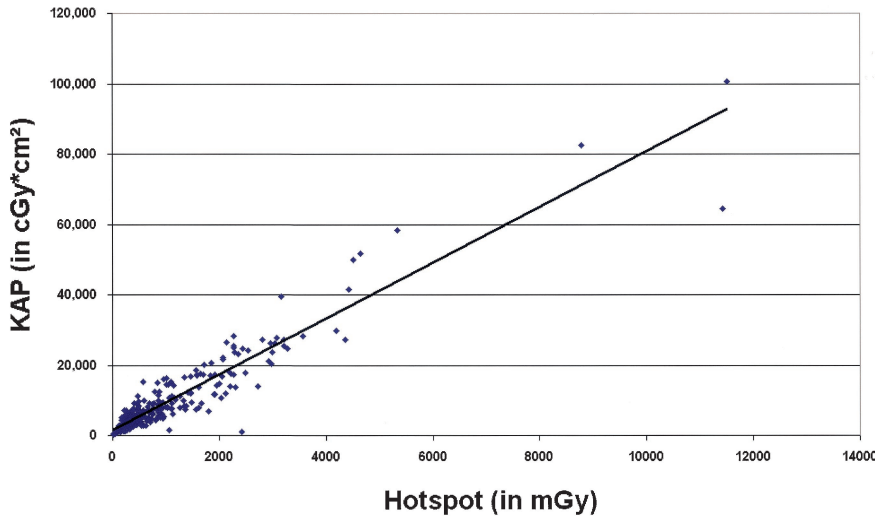


**Figure 6.** Correlation between high-dose area (hot spot) at skin and measured KAP for whole patient group was high:  $R=0.89$ ,  $x=1292.1$ ,  $y=7.947$ . Mean KAP was 52.19; mean high-dose area value was 0.475 Gy. With extreme values taken out (hot spot >4 Gy),  $R=0.81$ ,  $x=1299.9$ ,  $y=7.835$ .

**TABLE 3. Reported Radiobiological Effects of Radiation<sup>26–30</sup>**

	Threshold	Onset	Peak	Comments
Radiation-induced epilation				
Type				
Temporary	≈3 Gy	≈2 wk		New hair thinner
Permanent	≈7 Gy	≈2 wk		Protracted threshold ≈50 Gy
Radiation-induced erythema				
Reaction				
Early and transient	≈2 Gy	≈24 h		Not an indication for later response
Main effect	≈6 Gy	≈10 d	≈2 wk	Reddening ⇒ pigmentation >10 Gy pigment may last for months
Radiation-induced desquamation and ulceration				
Effect				
Dry desquamation	≈10 Gy	≈4 wk	≈5 wk	
Moist desquamation	≈15 Gy	≈4 wk	≈5 wk	Healing 2 weeks to months; late atrophy
Secondary	≈20 Gy	<6 wk		Dermal effect; ulceration secondary to sterilized basal cells
				Scarring

not apply to all patients, and ideally, a monitoring system should be tailored to the size of the patient. The actual size and location of irradiated skin parts may vary from one individual to another; future refinements to model the dimensions of individual patients more accurately would improve the accuracy of the skin dose distribution.

**Clinical Recommendations**

Our data show that the likelihood of high-dose areas may occur in the following circumstances: fluoroscopy time >60 minutes; gantry positioning unchanged throughout the procedure; and the irradiation occurring through a highly attenuating (eg, bone), thick body mass, requiring a high radiation quality during fluoroscopy and cinematography (>110 kVp). High-dose areas most likely occur when the left superior oblique projection is used.

**References**

1. Scott NS. Reports on 69 cases of injuries associated with rays, 6 of which were caused by the patients conditions, but most of which were burns caused by x rays. *Am X-Ray J.* 1897;1:57–66.
2. Calkins H, Niklason L, Sousa J, et al. Radiation exposure during radiofrequency catheter ablation of accessory atrioventricular connections. *Circulation.* 1991;6:2376–2382.
3. Cascade PN, Peterson LE, Wajszczuk WJ, et al. Radiation exposure to patients undergoing percutaneous transluminal coronary angioplasty. *Am J Cardiol.* 1987;9:996–997.
4. Huda W, Peters KR. Radiation-induced temporary epilation after a neuroradiologically guided embolization procedure. *Radiology.* 1994;193:642–644.
5. Kovoov P, Rieciardello M, Collins L, et al. Risk to patients from radiation associated with radiofrequency ablation for supraventricular tachycardia. *Circulation.* 1998;15:1534–1540.
6. Malkinson FD. Radiation injury to skin following fluoroscopically guided procedures. *Arch Dermatol.* 1996;6:695–696.
7. Geise RA, Peters NE, Dunnigan A, et al. Radiation dose during pediatric radiofrequency catheter ablation procedures. *Pacing Clin Electrophysiol.* 1996;11:1605–1611.

8. Karpinnen J, Parviainen T, Servomaa A, et al. Radiation risk and exposure of radiologists and patients during coronary angiography and percutaneous transluminal coronary angioplasty (PTCA). *Radiat Prot Dosimetry*. 1995;57:481–485.
9. Sovik E, Klow NE, Hellesnes J, et al. Radiation induced skin injury after percutaneous transluminal coronary angioplasty: case report. *Acta Radiol*. 1996;3:305–306.
10. Nahass GT. Acute radiodermatitis after radiofrequency catheter ablation. *J Am Acad Dermatol*. 1997;5:881–884.
11. Lichtenstein DA, Klapholz L, Vardy DA, et al. Chronic radiodermatitis following cardiac catheterization. *Arch Dermatol*. 1996;6:663–667.
12. D'Incan M, Roger H. Radiodermatitis following cardiac catheterization. *Arch Dermatol*. 1997;2:242–243.
13. Shope TB. Radiation-induced skin injuries from fluoroscopy. *Radiographics*. 1996;5:1195–1199.
14. Knautz MA, Abele DC, Reynolds TL. Radiodermatitis after transjugular intrahepatic portosystemic shunt. *South Med J*. 1997;3:352–356.
15. Den Boer A, de Feijter PJ, Hummel WA, et al. Reduction of radiation exposure while maintaining high-quality fluoroscopic images during interventional cardiology using novel x-ray tube technology with extra beam filtering. *Circulation*. 1994;6:2710–2714.
16. Pitney MR, Allan RM, Giles RW, et al. Modifying fluoroscopic views reduces operator radiation exposure during coronary angioplasty. *J Am Coll Cardiol*. 1994;7:1660–1663.
17. Food and Drug Administration. *Public Health Advisory. Avoidance of Serious X-ray Induced Skin Injuries to Patients During Fluoroscopically-Guided Procedures*. Rockville, Md: Center for Devices and Radiological Health, FDA: 1994, September 30.
18. Food and Drug Administration. *Important Information for Physicians and Other Healthcare Professionals: Recording Information in the Patient's Medical Record That Identifies the Potential for Serious X-ray Induced Skin Injuries Following Fluoroscopic Guided Procedures*. Rockville, Md: Center for Devices and Radiological Health, FDA: 1995, September 15.
19. Balter S. Guidelines for personnel radiation monitoring in the cardiac catheterization laboratory. Laboratory Performance Standards Committee of the Society for Cardiac Angiography and Interventions. *Cathet Cardiovasc Diagn*. 1993;4:277–279.
20. Vano E, Arranz L, Sastre JM at al. Dosimetric and radiation protection considerations based on some cases of patient skin injuries in interventional cardiology. *Br J Radiol*. 1998;845:510–516.
21. Sellers TD, Olley MC, DiLorenzo DR, et al. Radiation exposure during radiofrequency catheter ablation of accessory pathways. *Pacing Clin Electrophysiol*. 1992;15:582–584.
22. Bakalyar DM, Castellani MD, Safian RD. Radiation exposure to patients undergoing percutaneous transluminal coronary angioplasty. *Cathet Cardiovasc Diagn*. 1997;2:121–125.
23. Meier B. Radiation exposure in the cardiac catheterization laboratory: an issue or a non-issue? *Cathet Cardiovasc Diagn*. 1997;4:352.
24. Watson RM. Radiation exposure: clueless in the cath lab, or sayonara ALARA. *Cathet Cardiovasc Diagn*. 1997;2:126–127.
25. Zorzetto M, Bernardi G, Morrocutti G, et al. Radiation exposure to patients and operators during diagnostic catheterization and coronary angioplasty. *Cathet Cardiovasc Diagn*. 1997;4:348–351.
26. Radiation-induced skin injuries from fluoroscopy. *Food and Drug Administration Medical Bulletin*. 1994;24–26.
27. Pattee PL, Johns PC, Chambers RJ. Radiation risk to patient from percutaneous transluminal coronary angioplasty. *J Am Coll Cardiol*. 1993; 4:1044–1051.
28. Wagner LK, Eifel PJ, Geise RA. Potential biological effects following high x-ray dose interventional procedures. *J Vasc Interv Radiol*. 1994;1: 71–84.
29. Faulkner K, Love HG, Sweeny JK, et al. Radiation dose and somatic risk to patients during cardiac radiological procedures. *Br J Radiol*. 1986;700: 359–363.
30. Goldschmidt H, Sherwin WK. Reactions to ionizing radiation. *J Am Acad Dermatol*. 1980;6:551–579.